Theoretical study of the C_6H_3 potential energy surface and rate constants and product branching ratios of the $C_2H(^2\Sigma^+)+C_4H_2(^1\Sigma_g^+)$ and $C_4H(^2\Sigma^+)+C_2H_2(^1\Sigma_g^+)$ reactions

Alexander Landera,[1] Sergey P. Krishtal,[1] Vadim V. Kislov,[1] Alexander M. Mebel,[1,a)] and Ralf I. Kaiser[2]
[1]*Department of Chemistry and Biochemistry, Florida International University, 11200 SW 8th Street, Miami, Florida 33199, USA*
[2]*Department of Chemistry, University of Hawai'i at Manoa, Honolulu, Hawaii 96822-2275, USA*

(Received 20 March 2008; accepted 24 April 2008; published online 3 June 2008)

Ab initio CCSD(T)/cc-pVTZ//B3LYP/6-311G** and CCSD(T)/complete basis set (CBS) calculations of stationary points on the C_6H_3 potential energy surface have been performed to investigate the reaction mechanism of C_2H with diacetylene and C_4H with acetylene. Totally, 25 different C_6H_3 isomers and 40 transition states are located and all possible bimolecular decomposition products are also characterized. 1,2,3- and 1,2,4-tridehydrobenzene and $H_2CCCCCH$ isomers are found to be the most stable thermodynamically residing 77.2, 75.1, and 75.7 kcal/mol lower in energy than $C_2H+C_4H_2$, respectively, at the CCSD(T)/CBS level of theory. The results show that the most favorable $C_2H+C_4H_2$ entrance channel is C_2H addition to a terminal carbon of C_4H_2 producing HCCCHCCCH, 70.2 kcal/mol below the reactants. This adduct loses a hydrogen atom from the nonterminal position to give the HCCCCCCH (triacetylene) product exothermic by 29.7 kcal/mol via an exit barrier of 5.3 kcal/mol. Based on Rice–Ramsperger–Kassel–Marcus calculations under single-collision conditions, triacetylene+H are concluded to be the only reaction products, with more than 98% of them formed directly from HCCCHCCCH. The $C_2H+C_4H_2$ reaction rate constants calculated by employing canonical variational transition state theory are found to be similar to those for the related $C_2H+C_2H_2$ reaction in the order of magnitude of 10^{-10} cm^3 $molecule^{-1}$ s^{-1} for $T=298-63$ K, and to show a negative temperature dependence at low T. A general mechanism for the growth of polyyne chains involving $C_2H+H(C{\equiv}C)_nH \rightarrow H(C{\equiv}C)_{n+1}H+H$ reactions has been suggested based on a comparison of the reactions of ethynyl radical with acetylene and diacetylene. The $C_4H+C_2H_2$ reaction is also predicted to readily produce triacetylene+H via barrierless C_4H addition to acetylene, followed by H elimination. © *2008 American Institute of Physics*. [DOI: 10.1063/1.2929821]

INTRODUCTION

A better knowledge of the reactions of ground state ethynyl radicals, $C_2H(^2\Sigma^+)$, is of great importance for understanding the synthesis of complex hydrocarbon molecules in hydrocarbon-rich atmospheres of planets and their moons—predominantly of Titan.[1,2] Molecular nitrogen and methane are the main constituents of Titan's atmosphere, followed by hydrogen, nitrogen bearing molecules, and hydrocarbons.[3–9] Even though the unsaturated hydrocarbon molecules such as acetylene, ethylene, diacetylene, and benzene occur only in trace amounts of a few parts per 10^9,[10] they are of particular significance because they are thought to be the key intermediates to form Titan's organic, aerosol-particle based haze layers.[3] Ethynyl is considered as the key radical involved in the formation of the polyynes $CH_3(C{\equiv}C)_n$—H, H—$(C{\equiv}C)_n$—H, and H—$(C{\equiv}C)_n$ and in the complexation of the organic haze layers in Titan's atmosphere.[11–13] Whereas the main source of the ethynyl radicals has been unambiguously identified as the photolysis of acetylene (C_2H_2),[14–19] the underlying dynamics and kinetics of ethynyl radical reactions and the role in the buildup of complex hydrocarbons are far less clear. Based on chemical intuition, astrochemists and planetary chemists proposed that ethynyl radicals react with unsaturated hydrocarbons such as (substituted) alkynes via a hydrogen replacement to increase the complexity of the hydrocarbon [reactions (1) and (2)],[20–22]

$$C_2H + H(C{\equiv}C)_nH \rightarrow H(C{\equiv}C)_{n+1}H + H, \quad (1)$$

$$C_2H + CH_3(C{\equiv}C)_nH \rightarrow CH_3(C{\equiv}C)_{n+1}H + H. \quad (2)$$

These considerations have led to the development of photochemical models of Titan[23–28] and also to extensive laboratory studies during the past decades,[29,30] suggesting that either polyynes or aromatic hydrocarbon molecules are the dominant growth species of Titan's organic haze layer.

The simplest and prototype among the reactions [Eq. (1)], that of C_2H with acetylene,

a)Author to whom correspondence should be addressed. Electronic mail: mebela@fiu.edu.

$$C_2H + HC{\equiv}CH \rightarrow HC{\equiv}C-C{\equiv}CH + H, \quad (3)$$

has been extensively studied both experimentally and theoretically. For instance, the rate constants for C_2H disappearance in the $C_2H+C_2H_2$ reaction were measured in the temperature range of 170–350 K by Pedersen *et al.*,[31] between 295 and 450 K by Van Look and Peeters,[32] at 295–800 K by Ceursters *et al.*,[33] and at low temperatures down to 15 K by Chastaing *et al.*[34] All these studies showed that the reaction is fast and exhibits no or little temperature dependence on its rate coefficient, which was measured to be in the range of $(1.0–2.5)\times10^{-10}$ cm^3 molecule^{-1} s^{-1}, slightly increasing at low temperatures. Kaiser *et al.*[35] investigated chemical reaction dynamics of deuterated ethynyl C_2D with C_2H_2 in crossed molecular beams and identified two product channels; the major C_4HD+H (98–99%) and the minor C_4D+H_2 (1%–2%). They thus provided the first experimental proof that the ethynyl+acetylene reaction can indeed synthesize diacetylene. Theoretically, the $C_2H+C_2H_2$ reaction was studied using density functional B3LYP calculations by Kaiser *et al.*,[35] CCSD(T)//B3LYP calculations by Ceursters *et al.*,[33] and the most detailed study of the global C_4H_3 potential energy surface (PES) was performed by Le *et al.* at the G2M level.[36] These works agreed that the C_2H addition to C_2H_2 is barrierless, with all C_4H_3 intermediates and transition states along the most favorable reaction channel, leading to HCCCCH+H lying lower in energy than the initial reactants.

Very little is known about the mechanism and kinetics of the second reaction in series [Eq. (1)], C_2H+diacetylene, which accesses the C_6H_3 PES. Experimentally, the C_6H_3 radical was identified as a minor primary collisional photochemistry product of diacetylene triplet metastable state with acetylene, $C_4H_2^*+C_2H_2\rightarrow C_6H_3+H$, together with the major channel producing triacetylene, $C_4H_2^*+C_2H_2\rightarrow C_6H_2+2H$ (H_2).[37] Recently, cyclic *c*-C_6H_3 was shown to be produced in thermal dissociation of *ortho*-benzyne, *o*-$C_6H_4\rightarrow$*c*-C_6H_3+H, behind reflected shock waves under very isolated conditions.[38] The authors of this shock-tube study also inferred that in a secondary reaction channel, *c*-C_6H_3 isomerizes to a linear form and then loses a hydrogen atom to produce triacetylene: *c*-$C_6H_3\rightarrow$*l*-$C_6H_3\rightarrow C_6H_2+H$. Finally, a crossed molecular beam study of reactions of tricarbon molecules C_3 with C_3H_4 isomers, allene and methylacetylene, showed the formation of the 1-hexene-3,4-diynyl-2 radical $H_2CCCCCCH$ via atomic hydrogen elimination from a C_6H_4 intermediate as the major reaction channel.[39] Theoretically, to the best of our knowledge, only cyclic C_6H_3 isomers were investigated so far by high-level *ab initio* calculations,[40,41] prior to our recent work, in which we calculated geometries and relative energies of four different linear forms.[39] According to CCSD(T)/TZ2P//CCSD/DZP calculations by Bettinger *et al.*,[40] 1,2,4-tridehydrobenzene and 1,3,5-tridehydrobenzene are less stable than the 1,2,3-isomer by 4.0 and 11.8 kcal/mol, respectively.

The goal of the present study is to carefully investigate the mechanism of the $C_2H+C_4H_2$ reaction and the related $C_4H+C_2H_2$ reaction through detailed and chemically accurate calculations of various intermediates and transition states on the C_6H_3 PES. We also computed the thermal reaction rate constants at different temperatures using canonical variational transition state theory (CVTST). Also, in anticipation of future crossed molecular beam experiments under single-collision conditions, we calculated energy-dependent rate constants for individual unimolecular reaction steps on the C_6H_3 surface employing Rice–Ramsperger–Kassel–Marcus (RRKM) theory and computed reaction product branching ratios depending on collision energy. Finally, based on the results available for the $C_2H+C_2H_2$ and $C_2H+C_4H_2$ reactions, we speculate on the general mechanism of growth of polyynes via the C_2H-for-H exchange in $C_2H+H(C{\equiv}C)_nH$ encounters.

METHODS OF *AB INITIO* CALCULATIONS OF PES

Geometries of the reactants, products, and various intermediates and transition states on the C_6H_3 surface have been optimized at the hybrid density functional B3LYP level[42,43] with the 6-311G** basis set. Vibrational frequencies have been calculated using the same B3LYP/6-311G** method. Unscaled vibrational frequencies were used to calculate zero point energy (ZPE) corrections and reaction rate constants. To our experience, scaling of B3LYP frequencies does not significantly affect the relative energies of isomers and transition states and RRKM or VTST calculated rate constants. The optimized Cartesian coordinates, rotational constants, vibrational frequencies, and B3LYP/6-311G** total energies and ZPE for all species are given in the supplement to this paper.[44] Relative energies of the reactants, products, intermediates, and transition states have been refined utilizing the coupled cluster CCSD(T) method[45] with Dunning's correlation-consistent cc-pVTZ basis set.[46] Note that spin-restricted coupled cluster RCCSD(T) calculations were used for open-shell structures. For the most important species, we performed additional CCSD(T)/cc-pVDZ and CCSD(T)/cc-pVQZ calculations to extrapolate their CCSD(T) total energies to the complete basis set (CBS) limit by fitting the following equation:[47]

$$E_{\mathrm{tot}}(x) = E_{\mathrm{tot}}(\infty) + Be^{-Cx}, \quad (4)$$

where x is the cardinal number of the basis set [Eqs. (2)–(4)] and $E_{\mathrm{tot}}(\infty)$ is the CCSD(T)/CBS total energy. For the reactants and products, additional CCSD(T)/cc-pV5Z calculations were also feasible and the projection to the CBS limit was carried out more precisely using four CCSD(T) total energies with the cc-pVDZ, cc-pVTZ, cc-pVQZ, and cc-pV5Z basis sets. It should be noted that wherever comparison was possible, the relative energies obtained using CCSD(T)/CBS total energies from the three-point extrapolation (with the cc-pVDZ, cc-pVTZ, and cc-pVQZ basis sets) normally do not deviate from those computed from the four-point extrapolation by more than 0.1–0.2 kcal/mol (see Table I). We expect that our CCSD(T)/CBS+ZPE(B3LYP/6-311G**) relative energies should be accurate within 1 kcal/mol. For instance, for the C—H bond dissociation energy in acetylene, this method gives 131.4 kcal/mol, matching the experimental value of 131.3 ± 0.7 kcal/mol.[48] All *ab initio* and density functional

TABLE I. Relative energies (kcal/mol) of various fragment pairs in the C_6H_3 system with respect to $C_2H(X\,^2\Sigma^+)+C_4H_2(X\,^1\Sigma_g^+)$.

Fragment pair	Relative energy[a]	Precursors/initial adducts
$C_2H(^2\Sigma^+)+C_4H_2(^1\Sigma_g^+)$	0.0	1, 2, 3
$C_2H_2(^1\Sigma_g^+)+C_4H(^2\Sigma^+)$	1.7(1.7)	6, 21
$C_2(^1\Sigma_g^+)+C_4H_3(^2A')$	68.9(68.8)	5, 8
$C_2H_3(^2A')+l\text{-}C_4(^3\Sigma_g^-)$	77.0(76.8)	10
$c\text{-}C_3H_2(^1A_1)+c\text{-}C_3H(^2B_2)$	41.1(41.0)	20, 25
$c\text{-}C_3H_2(^1A_1)+l\text{-}C_3H(^2B_2)$	43.7(43.6)	21
$C_3H_3(^2B_1)+C_3(^1\Sigma_g^+)$	33.2(33.0)	9
$C(^3P)+H_2CCCCCH(^2B_1)$	60.8(60.8)	22, 23
$C(^3P)+HCCCHCCH(^2B_1)$	62.4(62.3)	18, 19
$CH(^2\Pi)+HCCCCCH(^3\Sigma_g^-)$	71.1(72.4)	2, 6
$CH_2(^3B_1)+l\text{-}C_5H(^2\Pi)$	68.9(68.8)	5, 7
$CH_3(^2A_2')+C_5(^1\Sigma_g^+)$	42.5(42.3)	11
$HCCCCCCH(^1\Sigma_g^+)+H$	−29.7(−29.6)	1, 6, 7
$H_2CCCCCC(^1A_1)+H$	19.9(19.7)	7, 11
meta-c-C_6H_2+H	4.2(3.9)	12, 14
ortho-c-C_6H_2+H	12.1(11.7)	12, 13
para-c-C_6H_2+H	18.8(18.5)	13
C_6H+H_2	2.1(2.0)	11

[a]Calculated at the CCSD(T)/CBS+ZPE(B3LYP/6-311G**) level with four-point extrapolation from CCSD(T)/cc-pVDZ, CCSD(T)/cc-pVTZ, CCSD(T)/cc-pVQZ, and CCSD(T)/cc-pV5Z energies. The numbers in parenthesis are obtained from three-point CBS extrapolation using CCSD(T)/cc-pVDZ, CCSD(T)/cc-pVTZ, and CCSD(T)/cc-pVQZ energies.

calculations have been performed using the GAUSSIAN-98 (Ref. 49) and MOLPRO 2002 (Ref. 50) program packages.

RESULTS AND DISCUSSION

C_6H_3 potential energy surface

The overall map of the C_6H_3 PES including all calculated intermediates and transition states is depicted in Fig. 1, where we show the relative energies of various species calculated at the CCSD(T)/cc-pVTZ+ZPE(B3LYP/6-311G**) level. The potential energy profile for the most important channels of the $C_2H+C_4H_2$ and $C_4H+C_2H_2$ reactions is illustrated in Fig. 2; here, we show higher-level CCSD(T)/CBS+ZPE relative energies. The $C_2H+C_4H_2$ reaction starts by a barrierless addition of ethynyl to a carbon atom of diacetylene. The addition to a terminal carbon is more thermodynamically favorable and produces a chain intermediate 1, HCCCHCCCH, residing 63.9 and 70.2 kcal/mol lower in energy than the initial reactants at the CCSD(T)/cc-pVTZ and CCSD(T)/CBS levels of theory, respectively (here and below ZPE corrections calculated at B3LYP/6-311G** are included in the relative energies). The alternative addition to a middle carbon leads to a branched isomer 2, HCCC(CH)CCH, also without an entrance barrier but with lower exothermicities of 53.3 and 53.9 kcal/mol at CCSD(T)/cc-pVTZ and CCSD(T)/CBS, respectively. The adducts 1 and 2 are connected to one another by migration of the C_2H group over a triple bond in the diacetylene fragment via a cyclic intermediate 3. Structure 3 resides 37.8 kcal/mol below the reactants and the barriers for the $2\rightarrow3$ and $3\rightarrow1$

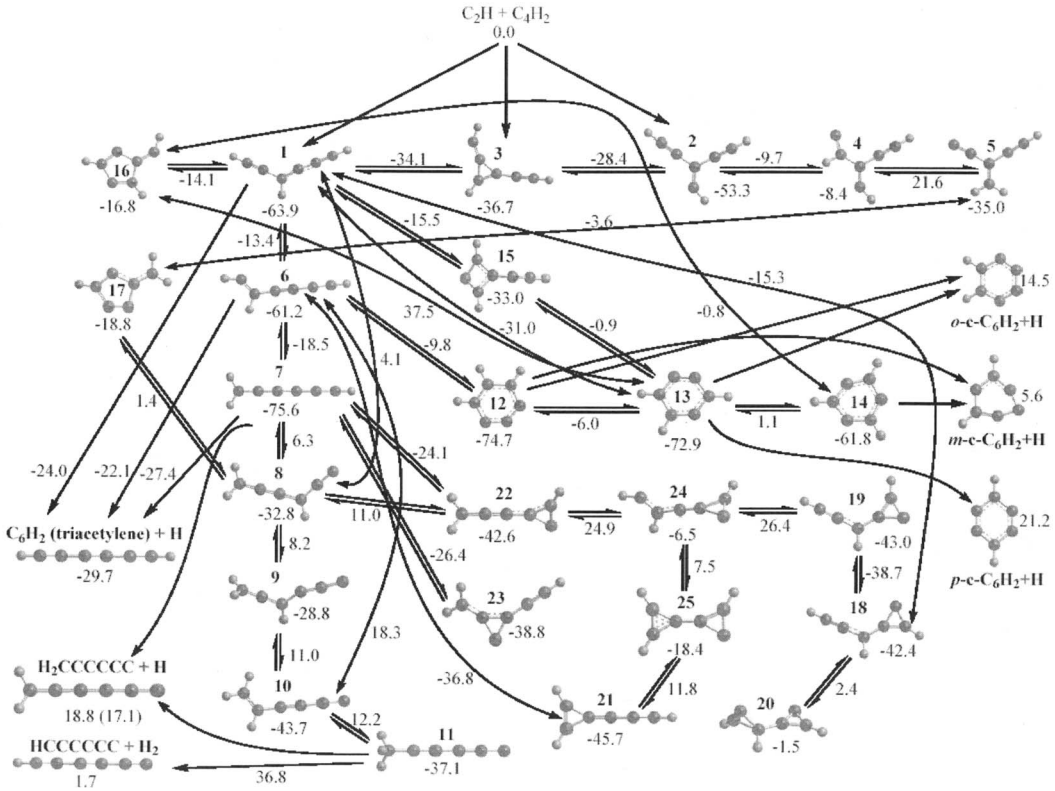

FIG. 1. Potential energy map of the C_6H_3 system. The numbers show relative energies (in kcal/mol) of various C_6H_3 isomers and transition states as well as fragment pairs calculated at the CCSD(T)/cc-pVTZ//B3LYP/6-311G**+ZPE(B3LYP/6-311G**) level of theory.

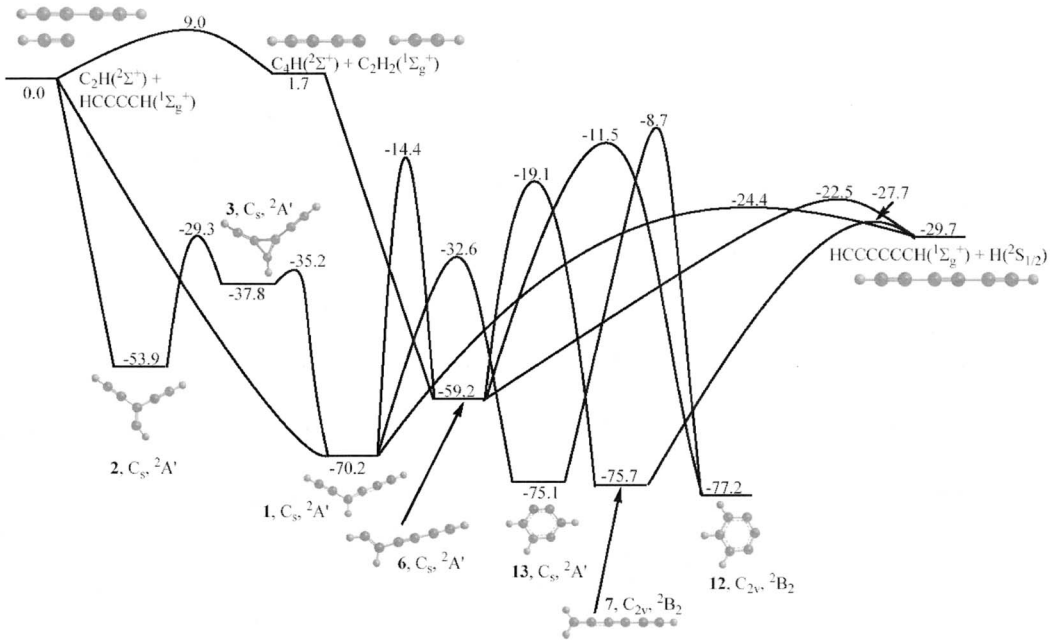

FIG. 2. Potential energy profile for the most favorable channels of the $C_2H+C_4H_2$ and $C_4H+C_2H_2$ reactions calculated at the CCSD(T)/CBS//B3LYP/6-311G**+ZPE(B3LYP/6-311G**) level. The numbers indicate relative energies (in kcal/mol) of various species in kcal/mol.

rearrangements involving the C_2H shifts are calculated to be 24.6 and 2.6 kcal/mol, respectively, at the CCSD(T)/CBS level. According to the PES scan from the initial reactants toward 1, 2, and 3, descending trajectories exist, leading to all three initial adducts; however, the minimal energy pathway leads the system to isomer 1, the most stable of the three. In any case, one can see that the cyclic structure 3 is only metastable with regard to the ring opening producing 1, whereas 2 is also likely to rearrange to 1 because the highest in energy transition state (TS) on the $2\rightarrow3\rightarrow1$ pathway lies 29.3 kcal/mol below the reactants. An alternative pathway for isomerization of 2 is not favorable. In principle, this intermediate can undergo two consecutive H migrations, leading to another branched isomer 5, $CCC(CH_2)CCH$, residing 35.0 kcal/mol below $C_2H+C_4H_2$ at the CCSD(T)/cc-pVTZ level via intermediate 4. However, the TS between 4 and 5 lies 21.6 kcal/mol above the reactants, making this process highly unlikely. Structure 4 exists as a local minimum only at the B3LYP/6-311G** level; at CCSD(T)/cc-pVTZ, its energy becomes slightly higher than that of TS for $2\rightarrow4$. We conclude that the $2(\rightarrow4)\rightarrow5$ channel can be safely ruled out for the $C_2H+C_4H_2$ reaction, although 5 may play a role of the initial adduct in the $C_2+i\text{-}C_4H_3$ and $CH_2+l\text{-}C_5H$ reactions.

The HCCCHCCCH intermediate 1 can lose the H atom from the central carbon to form the triacetylene+H products. Overall, the $C_2H+HCCCCH\rightarrow1\rightarrow HCCCCCCH+H$ reaction is calculated to be 29.7 kcal/mol exothermic. The barrier for the H loss from 1 is 45.8 kcal/mol at the CCSD(T)/CBS//B3LYP level and the reverse barrier for H addition to a central carbon of triacetylene is thus 5.3 kcal/mol. It is well known that calculations using B3LYP optimized geometries of TS for H losses tend to slightly underestimate the H elimination barriers because the length of the breaking C—H bond in such TSs is normally overestimated by B3LYP.[51] More accurate TS geometries and energies can be obtained by employing the intrinsic reaction coordinate maximum (IRCMax) approach,[52] in which the energies of various structures along the minimal energy reaction pathway in the TS vicinity obtained by lower level intrinsic reaction coordinate calculations (in this case by B3LYP) are recomputed at a higher theoretical level, such as CCSD(T)/CBS. Malick *et al.* suggested that the IRCMax TS geometry tends to converge to the optimized high-level geometry.[52] For the $H+C_2H_2$ reaction, analogous to the H addition to triacetylene, Sayes *et al.*[51] compared IRCMax[CBS-QB3//B3LYP/6-311G(d,p)] and B3LYP/6-311G(d,p) TS geometries and found the C—H distance for the forming bond in the former to be 0.112 Å shorter than in the latter. However, due to the flatness of the PES in the TS region, the H addition barrier calculated at IRCMax[CBS-QB3//B3LYP/6-311G(d,p)] is only 0.3 kcal/mol higher than the CBS-QB3//B3LYP/6-311G(d,p) value. To evaluate a possible error bar in the H elimination barriers owing to this phenomenon, we performed IRCMax[CCSD(T)/CBS//B3LYP/6-311G(d,p)] calculations of the TS for the H loss from 1. Here, the effect appeared to be somewhat stronger, although still minor. The breaking C—H bond length decreases from 1.987 Å at B3LYP to 1.818 Å at IRCMax and the TS relative energy increases by 0.95 to −23.45 kcal/mol. We can conclude that the CCSD(T)/CBS//B3LYP/6-311G(d,p) H elimination barriers are likely underestimated by ~1 kcal/mol.

Besides the H loss, 1 can be subjected to isomerization processes, including a variety of H migrations and ring closures. We first consider hydrogen shifts leading to different chain isomers of the C_6H_3 radical. The 3,2-H shift in 1 (in the chain isomers, we numbered carbon atoms from left to right, as shown in Figs. 1 and 2) leads to intermediate 6,

HCCHCCCCH, 59.2 kcal/mol below the reactants at CCSD(T)/CBS, over a high barrier of 55.8 kcal/mol. Still, the H migration TS lies 14.4 kcal/mol lower in energy than $C_2H+C_4H_2$. Structure 6 can eliminate the H atom from the carbon in position 2 to produce triacetylene; in this case, the H loss barrier is 36.7 kcal/mol relative to 6, and the reverse H addition barrier is 7.2 kcal/mol. Next, 2,1-H migration in 6 generates isomer 7, the C_{2v}-symmetric 1-hexene-3,4-diynyl-2 radical $H_2CCCCCCH$ ($^2B_2$). Structure 7 is one of the most stable C_6H_3 isomers and resides 75.7 kcal/mol lower in energy than the reactants at the CCSD(T)/CBS level. The 2,1-H shift barrier from 6 to 7 is calculated to be 40.1 kcal/mol. The 1-hexene-3,4-diynyl-2 radical is the third precursor of triacetylene on the C_6H_3 PES, along with 1 and 6. For 7, the H loss barrier to produce HCCCCCCH is 48.0 kcal/mol and the reverse H addition barrier is only 2.0 kcal/mol. Thus, in accordance with Hummond's rule, the H addition to triacetylene is most favorable to the terminal carbon atom with the barrier of 2.0 kcal/mol and the highest exothermicity of 46.0 kcal/mol, followed by the addition to a central C (in position 3) leading to 1 (barrier 5.3 kcal/mol, exothermicity of 40.5 kcal/mol), and then by addition to a carbon in position 2 (barrier 7.2 kcal/mol, exothermicity of 29.5 kcal/mol). In principle, $H_2CCCCCCH$ may also eliminate H from the terminal CH group yielding the $H_2CCCCCC$ isomer of C_6H_2. However, this structure is much less stable than triacetylene; the $H_2CCCCCC+H$ products lie 19.9 kcal/mol above $C_2H+C_4H_2$ at the CCSD(T)/CBS level and their formation is improbable.

Further H migrations in 7 are theoretically possible but unlikely. For instance, 6,4-H shift would lead to isomer 8, $H_2CCCCHCC$, 32.8 kcal/mol below the reactants at the CCSD(T)/cc-pVTZ level. However, the barrier for such rearrangement is high, 81.9 kcal/mol, and the corresponding TS is 7.0 kcal/mol higher in energy than the reactants. Structure 8 can also be produced directly from 1 through 6,1-H migration but again the barrier is too high and the respective TS lies 4.1 kcal/mol above $C_2H+C_4H_2$. Therefore, structure 8 should not be relevant to the reaction of ethynyl with diacetylene; alternatively, this isomer can be produced as an initial adduct of the C_2+i-C_4H_3 and H_2CCC+l-C_3H reactions. The 4,3-H shift in 8 brings forth intermediate 9, $H_2CCCHCCC$, with the relative energy of −28.8 kcal/mol. Again, the H migration barrier is prohibitively high with the corresponding TS residing 8.2 kcal/mol above the reactants at the CCSD(T)/cc-pVTZ level. Structure 9 should not be important for the $C_2H+C_4H_2$ reaction but can be formed, in principle, by the addition of tricarbon C_3 to the propargyl radical C_3H_3. In turn, isomer 9 can be subjected to another 3,2-H shift to produce intermediate 10, $H_2CCHCCCC$, 43.7 kcal/mol below the reactants, over a barrier with the TS lying 11.0 kcal/mol above the reactants. Structure 10 can also be formed by 6,1-H shift in 6, but the respective TS is even higher in energy, 18.3 kcal/mol above $C_2H+C_4H_2$. Although irrelevant to the reaction of ethynyl with diacetylene, 10 may play a role of the initial intermediate in the reaction of C_2H_3 with l-C_4. Finally, 2,1-H shift in 10 gives isomer 11, $H_3CCCCCC$, whose relative energy is −37.1 kcal/mol. The H migration barriers are calculated to be 55.9 and 12.2 kcal/mol relative to 10 and the reactants, respectively. Possible dissociation pathways of 11 include atomic and molecular hydrogen eliminations; $H_2CCCCCC+H$ and $HCCCCCC+H_2$. Overall, these product channels are endothermic by 19.9 and 2.1 kcal/mol relative to $C_2H+C_4H_2$, respectively, and the H_2 loss pathway proceeds via a high barriers of 73.9 and 36.8 kcal/mol with respect to 11 and the reactants. $H_3CCCCCC$ 11 and its decomposition products are not expected to be accessed through the reaction of ethynyl with diacetylene but 11 can serve as a gateway for the CH_3+l-C_5 reaction.

In addition to the chain C_6H_3 isomers considered above, another group of rather stable intermediates includes six-member rings, 1,2,3-, 1,2,4-, and 1,3,5-tridehydrobenzenes, 12, 13, and 14, respectively. The most favorable of them is 1,2,3-tridehydrobenzene 12, which resides 77.2 and 74.7 kcal/mol lower in energy than $C_2H+C_4H_2$ at the CCSD(T)/CBS and CCSD(T)/cc-pVTZ levels, respectively. At our best CCSD(T)/CBS level, 12 is 1.5 kcal/mol lower in energy than the most stable chain isomer 1-hexene-3,4-diynyl-2 7, whereas at CCSD(T)/cc-pVTZ, the latter is slightly more favorable than 12 by 0.9 kcal/mol. 1,2,4-tridehydrobenzene 13 is also close in energy to 12 and 7; at CCSD(T)/CBS, it lies 2.1 and 0.6 kcal/mol above those two structures, respectively. We conclude that 1,2,3- and 1,2,4-tridehydrobenzenes and 1-hexene-3,4-diynyl-2 are the most thermodynamically preferable C_6H_3 isomers with 1,2,3-tridehydrobenzene 12 being the global minimum on the C_6H_3 PES, at least according to the most accurate at present CCSD(T)/CBS calculations. 1,3,5-tridehydrobenzene 14 is significantly less favorable; at the CCSD(T)/cc-pVTZ level, it lies 61.8 kcal/mol below the reactants.

1,2,4-tridehydrobenzene 13 can be formed from 1 by three different mechanisms, one-step six-member ring closure, two-step four-member ring closure to intermediate 15 followed by four-to-six ring expansion of the latter, and two-step five-member ring closure to isomer 16, followed by its five-to-six ring expansion. The direct one-step channel is energetically preferable as the barriers for the $1 \rightarrow 13$ rearrangement are 32.9 and 37.6 kcal/mol at the CCSD(T)/cc-pVTZ and CCSD(T)/CBS levels, respectively. The four-member ring closure $1 \rightarrow 15$ requires a barrier of 48.4 kcal/mol at CCSD(T)/cc-pVTZ, whereas the ring expansion $15 \rightarrow 13$ occurs via a 32.1 kcal/mol barrier. At the same CCSD(T)/cc-pVTZ level, the highest in energy TS on the two-step $1 \rightarrow 15 \rightarrow 13$ pathway lies only 0.2 kcal/mol lower in energy than the initial reactants, whereas the TS for the direct $1 \rightarrow 13$ process is 31.0 kcal/mol below $C_2H+C_4H_2$. The third pathway via the five-member ring intermediate 16 is clearly unfavorable, as the TS corresponding to the second ring-expansion $16 \rightarrow 13$ step lies as high as 37.5 kcal/mol above the reactants. Structure 16 is more likely to undergo ring expansion to 1,3,5-tridehydrobenzene 14, overcoming a much lower barrier of 17.6 kcal/mol (0.8 kcal/mol below $C_2H+C_4H_2$). The $1 \rightarrow 16 \rightarrow 13/14$ pathways are not expected to play any significant role in the reaction mechanism because the direct rearrangement of 1–13 and the H loss in 1 exhibit significantly lower barriers than that for the five-member ring closure to form 16. 1,2,3-tridehydrobenzene 12

can be produced by the ring closure in intermediate 6 over a barrier of 47.7 kcal/mol [CCSD(T)/CBS]. The three tridehydrobenzenes are connected to each other by 1,2-H migrations, $12 \rightarrow 13 \rightarrow 14$, with the barriers of 68.7 and 74.0 kcal/mol for the first and second steps, respectively. The H migration barriers are significantly higher than those for the ring openings $12 \rightarrow 6$ and especially $13 \rightarrow 1$ and, therefore, the H shifts in six-member rings are expected to be slow and are not anticipated to play any significant role. Direct H elimination from 12, 13, and 14 lead to the cyclic isomers of C_6H_2, *ortho-*, *meta-*, and *para-*tetradehydrobenzenes: $12 \rightarrow o\text{-}c\text{-}C_6H_2+H$, $12 \rightarrow m\text{-}c\text{-}C_6H_2+H$, $13 \rightarrow o\text{-}c\text{-}C_6H_2+H$, $13 \rightarrow p\text{-}c\text{-}C_6H_2+H$, and $14 \rightarrow m\text{-}c\text{-}C_6H_2+H$. However, the relative energies of these products with respect to the $C_2H+C_4H_2$ reactants are rather high, 4.2, 12.1, and 18.8 kcal/mol for $m\text{-}c\text{-}C_6H_2$, $o\text{-}c\text{-}C_6H_2$, and $p\text{-}c\text{-}C_6H_2$, respectively, at the CCSD(T)/CBS level. Thus, at this level of theory, the *m-*, *o-*, and *p*-cyclic C_6H_2 isomers are 33.9, 41.8, and 48.5 kcal/mol less stable than triacetylene (note that earlier Bettinger *et al.* obtained the energies of *m-*, *o-*, and *p*-tetradehydrobenzenes relative to triacetylene as 38, 43.2, and 49 kcal/mol, respectively, at the CCSD(T)/TZ2P//CCSD/DZ+ZPE(B3LYP/6-31G*) level[40]). Therefore, instead of losing an atomic hydrogen, tridehydrobenzenes are more likely to undergo ring openings to the chain intermediates 1 or 6 and then split an H atom to produce triacetylene. This result agrees with the recent experimental observation by Xu *et al.*, who deduced from their shock-tube measurements of thermal dissociation of *o*-benzyne that the primary cyclic C_6H_3 products rearrange to linear C_6H_3 before decomposing to triacetylene+H.[38]

Besides isomer 16, we found another five-member ring local minimum 17, which possesses an out-of-ring CH_2 group. Structure 17 resides 18.8 kcal/mol below $C_2H+C_4H_2$ and can be formed by ring closures in isomers 5 and 8 via TSs lying 3.6 and 2.1 kcal/mol lower in energy than the reactants, respectively. Since the formation of 5 and 8 in the $C_2H+C_4H_2$ reaction is hindered by high barriers at TSs $4 \rightarrow 5$, $7 \rightarrow 8$, and $1 \rightarrow 8$, 17 (like 16) is not likely to be accessed. On the other hand, this intermediate could be produced in the reaction of C_2 with $i\text{-}C_4H_3$ leading directly to the structure 5 or 8. We tried to find a TS directly connecting two five-member ring isomers 16 and 17 by a 1,3-H shift from the out-of-ring carbon to the neighboring C atom in the C_5 cycle. However, such saddle-point search instead converged to the $1 \rightarrow 8$ TS.

The last group of C_6H_3 isomers includes three-member ring structures 18–25. For instance, three-member ring closure in 1 leads to intermediate 18 with a HCCCH group attached to a C_3H cycle. The calculated barrier for this process is 48.6 kcal/mol relative to 1 at the CCSD(T)/cc-pVTZ level and 18 resides 42.4 kcal/mol below the reactants. Structure 19 is another conformer of 18, which is almost isoergic with the latter. The two structures 18 and 19 are connected by rotation around the out-of-ring C—C bond via a low barrier of 3.7 kcal/mol relative to 18. Structure 18 can also undergo the second ring closure leading to structure 20 with two three-member rings C_3H_2 and C_3H linked to each other. Structure 20 lying 1.5 kcal/mol lower in energy than $C_2H+C_4H_2$, is only a metastable intermediate because the barrier for the reverse $20 \rightarrow 18$ ring opening is as low as 3.9 kcal/mol. Ring closure in structure 6 proceeding over a relatively low barrier of 24.4 kcal/mol (36.8 kcal/mol below the initial reactants) results in C_{2v}-symmetric isomer 21, which has a linear C_3H group attached to a C_3H_2 cycle. Structure 21 is the most stable among all three-member ring intermediates and resides 45.7 kcal/mol lower in energy than $C_2H+C_4H_2$. 1-hexene-3,4-diynyl-2 7 can ring close to two different three-member ring isomers, $H_2CCC\text{-}(c\text{-}C_3H)$ 22 and $(c\text{-}C_3)(CH_2)(C_2H)$ 23. The barriers calculated for both ring closures are similar, 51.5 and 51.3 kcal/mol relative to 7, respectively. The relative energies of 22 and 23, −42.6 and −38.8 kcal/mol, are also close. 1,2-H shift in 22 leads to intermediate 24, $CHCHC\text{-}(c\text{-}C_3H)$ residing 6.5 kcal/mol below $C_2H+C_4H_2$. Alternatively, 24 can be produced by 3,2-H migration in 19. However, the barriers for both $22 \rightarrow 24$ and $19 \rightarrow 24$ processes are calculated to be high, with the corresponding transition states lying 24.9 and 26.4 kcal/mol above $C_2H+C_4H_2$. In principle, 24 can undergo a second three-member ring closure to form another bicyclic intermediate 25 via a barrier of 14.0 kcal/mol. C_s-symmetric 25 lies 18.4 kcal/mol below the initial reactants and possesses two coplanar C_3H_2 and C_3H rings linked by a C—C bond; in contrast to the other bicyclic structure 20, the C—C bridge in 25 has no H atoms attached. Finally, intermediate 25 can also be produced by ring closure in 21 overcoming a barrier of 57.6 kcal/mol (11.8 kcal/mol relative to the reactants). The three-member ring structures 18–25 cannot directly lose a hydrogen atom to form any viable C_6H_2 isomer and, therefore, this area of the C_6H_3 PES, though energetically accessible in the $C_2H+C_4H_2$ reaction, represents a "dead end" on the surface and their role in the reaction mechanism is not expected to be considerable. The three-member cyclic structures can be alternatively reached by some other bimolecular encounters; for instance, 18 and 19 can be formed in the reactions of propargylene HCCCH with cyclic C_3H and atomic carbon with the C_5H_3 isomer HCCCHCCH, 20 and 25 can be produced from $c\text{-}C_3H_2$ and $c\text{-}C_3H$, 21 from $c\text{-}C_3H_2$ and linear $l\text{-}C_3H$, 22 and 23 from C and $H_2CCCCCCH$, and 22 also from vinylidenecarbene H_2CCC and $c\text{-}C_3H$.

The most favorable channels of the $C_2H+C_4H_2$ reaction

Having investigated the broad variety of C_6H_3 local minima and transition states, we are now in position to summarize the most favorable mechanism of the $C_2H+C_4H_2$ reaction illustrated in Fig. 2. The reaction starts by barrierless formation of isomer 1 or 2, or some descending trajectories can lead to the cyclic adduct 3. Nevertheless, both 2 and 3 will preferably isomerize to 1 unless they can be stabilized by collisions. Structure 1 loses an H atom to produce triacetylene HCCCCCCH via a barrier of 45.8 kcal/mol and the products are 29.7 kcal/mol exothermic as compared to the reactants. Alternatively, 1 can undergo H migrations to 6 over a barrier of 55.8 kcal/mol and then to the most stable C_6H_3 isomer 7, $H_2CCCCCCH$, overcoming a 51.1 kcal/mol

TABLE II. Calculated product branching ratios of the $C_2H+C_4H_2$ and $C_4H+C_2H_2$ reactions under single-collision conditions at different collision energies E_{col}.

E_{col} (kcal/mol) product	0.0	1.0	2.0	3.0	4.0	5.0	6.0	7.0	8.0	9.0	10.0
$C_2H+HCCCCH$											
C_6H_2+H via 1	99.41	99.32	99.23	99.12	99.01	98.90	98.78	98.66	98.53	98.40	98.26
C_6H_2+H via 6	0.41	0.47	0.54	0.61	0.68	0.75	0.83	0.91	0.99	1.08	1.17
C_6H_2+H via 7	0.17	0.20	0.24	0.27	0.31	0.35	0.39	0.43	0.48	0.53	0.58
$C_4H+C_2H_2$											
C_6H_2+H via 1	1.28	1.42	1.56	1.70	1.85	2.00	2.15	2.30	2.46	2.61	2.77
C_6H_2+H via 6	68.64	68.17	67.72	67.29	66.87	66.47	66.08	65.71	65.35	65.01	64.68
C_6H_2+H via 7	30.07	30.41	30.72	31.01	31.28	31.54	31.77	31.99	32.19	32.37	32.55

barrier with respect to 1. Both 6 and 7 can also split a hydrogen atom and produce triacetylene with barriers of 47.7 and 42.5 kcal/mol relative to 1. Ring closure in 1 and 6 to form 1,2,4- and 1,2,3-tridehydrobenzenes 13 and 14 is also feasible and occurs with barriers of 37.6 and 58.7 kcal/mol relative to the initial adduct 1. However, since six-member ring C_6H_2 isomers are high in energy, the tridehydrobenzenes would rearrange to the chain structures 1, 6, and 7 rather than decompose. Thus, if collisional stabilization does not occur, the only competitive reaction channels are $C_2H+C_4H_2 \rightarrow \cdots \rightarrow 1 \rightarrow C_6H_2$ (triacetylene)$+H$, $C_2H+C_4H_2 \rightarrow \cdots \rightarrow 1 \rightarrow 6 \rightarrow C_6H_2+H$, and $C_2H+C_4H_2 \rightarrow \cdots \rightarrow 1 \rightarrow 6 \rightarrow 7 \rightarrow C_6H_2+H$. The formation of the $H_2CCCCCC$ isomer of C_6H_2 by H loss from 7 or 11 is not expected to occur because of high endothermicity of the products. The $HCCCCCC+H_2$ fragments are slightly endothermic but their formation via 11 is not likely because of prohibitively high barriers on the pathway leading to 11 from 1 and for the molecular hydrogen elimination from 11. Despite a careful search, we could not find a first-order saddle point for the H_2 lost from intermediate 7. As seen from Table I, all other possible reaction products are highly endothermic, except $C_4H+C_2H_2$, which are endothermic by 1.7 kcal/mol but lie 31.4 kcal/mol higher in energy than triacetylene+H. The direct hydrogen abstraction reaction, $C_2H+C_4H_2 \rightarrow C_2H_2+C_4H_2$, is also unlikely to compete unless collision energy or temperature are very high because, in contrast to barrier-free and highly exothermic C_2H addition to diacetylene, it exhibits a sizable barrier of 9.0 kcal/mol. Thus, $HCCCCCCH+H$ are predicted to be the exclusive products of the reaction of ethynyl radical with diacetylene.

The only remaining issue, what are the relative yields of triacetylene directly from 1 and from 6 and 7, is addressed by RRKM calculations of energy-dependent rate constants for individual unimolecular steps and branching ratios of different channels. The computational procedure for these calculations has been described in our previous works in detail.[53] We calculated rate constants as functions of available internal energy of each intermediate or TS, the internal energy was taken as a sum of the energy of chemical activation in the $C_2H+C_4H_2$ reaction and the collision energy, assuming that a dominant fraction of the latter is converted to an internal vibrational energy. The harmonic approximation was used in calculations of numbers and densities of state. With all rate constants in hand, we computed product branching ratios by solving first-order kinetic equations for unimolecular reactions according to the reaction scheme shown in Fig. 2. Only a single total-energy level was considered throughout, as for single-collision conditions (zero-pressure limit). We employed the fourth-order Runge–Kutta method to solve the equations; the product concentrations at the time when they converged were used to compute branching ratios. As seen in Table II, according to our RRKM calculations, more than 98% of the C_6H_2+H products are formed via decomposition of intermediate 1, although this fraction slightly decreases as collision energy grows. Only trace amounts are produced either from 6 or 7.

The most favorable channels of the $C_2H_2+C_4H$ reaction

The butadiynyl radical, CCCCH ($^2\Sigma^+$), adds to a carbon atom of acetylene also without a barrier to produce intermediate 6 with exothermicity of 60.9 kcal/mol. Structure 6 either directly loses a hydrogen atom yielding triacetylene or isomerizes to 1 or 7 by H migrations. The H loss and migration barriers with respect to 6 are calculated to be 36.7, 44.8, and 40.1 kcal/mol, respectively. Intermediates 1 and 7 also produce $HCCCCCCH+H$ via respective barriers of 34.8 and 31.5 kcal/mol relative to 6. Thus, triacetylene+H are exclusive products of the reaction of C_4H radicals with acetylene and the competitive reaction scenarios are $C_2H_2+C_4H \rightarrow 6 \rightarrow C_6H_2+H$, $C_2H_2+C_4H \rightarrow 6 \rightarrow 7 \rightarrow C_6H_2+H$, and $C_2H_2+C_4H \rightarrow 6 \rightarrow 1 \rightarrow C_6H_2+H$. According to RRKM calculations of branching ratios for these channels (Table II), about 2/3 of the products are formed by direct decomposition of 6 and 1/3 is produced from 7. A small amount of C_6H_2+H, 1%–3%, are formed via 1; this fraction slightly increases with collision energy. We can conclude that although the $C_2H+C_4H_2$ and $C_4H+C_2H_2$ reactions will produce the same triacetylene+H products, their dynamics may be different owing to the distinction in the decomposing C_6H_3 complexes.

Unimolecular decomposition of cyclic C_6H_3

According to the recent experimental shock-tube studies by Xu *et al.*,[38] unidentified *c*-C_6H_3 isomers were formed as primary products of thermal decomposition of *ortho*-

benzyne, *o*-C_6H_4. H eliminations from the latter can give either 1,2,4-tridehydrobenzene 13 or 1,2,3-tridehydrobenzene 14. Xu *et al.* also concluded that secondary decomposition of *c*-C_6H_3 leads to triacetylene by an H loss, following rearrangement of the cyclic structures to a linear C_6H_3 isomer. The present calculations of the C_6H_3 PES support this conclusion. As the energies of cyclic C_6H_2 isomers are much higher than that of HCCCCCCH, the most favorable scenarios of unimolecular decomposition of 13 and 14 are respectively the following: 13→ring opening (barrier of 42.5 kcal/mol)→1→H elimination (barrier of 50.7 kcal/mol relative to 13)→C_6H_2 (triacetylene)+H and 14→ring opening (barrier of 65.7 kcal/mol)→6→H elimination (barrier of 52.8 kcal/mol relative to 14)→C_6H_2 (triacetylene)+H as well as 14→6→H migration (barrier of 58.1 kcal/mol relative to 14)→7→H elimination (barrier of 49.5 kcal/mol)→C_6H_2 (triacetylene)+H. Interestingly, cyclic C_6H_3 is the first species in the row C_6H_6 (benzene), C_6H_5 (phenyl), C_6H_4 (benzyne), C_6H_3 (tridehydrobenzene), for which H elimination is accompanied by destruction of the C_6 aromatic ring; benzene preferably decomposes to phenyl+H,[53,54] phenyl radical predominantly produces *o*-benzyne+H,[55] whereas for *o*-benzyne the most favorable dissociation products are diacetylene C_4H_2 +acetylene,[56] but the H loss leading to cyclic C_6H_3 is a sizable minor channel.[38]

Other possible reactions on the C_6H_3 surface

All possible bimolecular fragments of C_6H_3 are summarized in Table I. One can see that all of them are highly endothermic as compared to triacetylene+H. Therefore, C_6H_2+H are expected to be exclusive products of all the reactions listed in this table, unless energetically favorable C_6H_3 isomers, such as tridehydrobenzenes and 1-hexene-3,4-diynyl-2 can be collisionally stabilized. The potential energy map in Fig. 1 helps to predict the most energetically favorable reaction channels:

$$C_2(^1\Sigma_g^+) + C_4H_3(^2A') \rightarrow (5 \rightarrow 17 \rightarrow)8 \rightarrow 1 \rightarrow C_6H_2 + H, \quad \Delta E = -98.6 \text{ kcal/mol},$$

$$C_2H_3(^2A') + l - C_4(^3\Sigma_g^-) \rightarrow 10 \rightarrow 9 \rightarrow 8 \rightarrow 1 \rightarrow C_6H_2 + H, \quad \Delta E = -106.7 \text{ kcal/mol},$$

$$c - C_3H_2(^1A_1) + c - C_3H(^2B_2) \rightarrow 25 \rightarrow 21 \rightarrow 6 \rightarrow C_6H_2 + H, \quad \Delta E = -70.8 \text{ kcal/mol},$$

$$c - C_3H_2(^1A_1) + 1 - C_3H(^2B_2) \rightarrow 21 \rightarrow 6 \rightarrow C_6H_2 + H, \quad \Delta E = -73.4 \text{ kcal/mol},$$

$$C_3H_3(^2B_1) + C_3(^1\Sigma_g^+) \rightarrow 9 \rightarrow 8 \rightarrow 1 \rightarrow C_6H_2 + H, \quad \Delta E = -62.9 \text{ kcal/mol},$$

$$C(^3P) + H_2CCCCCH(^2B_1) \rightarrow 22 \text{ or } 23 \rightarrow 7 \rightarrow C_6H_2 + H, \quad \Delta E = -90.5 \text{ kcal/mol},$$

$$C(^3P) + HCCCHCCH(^2B_1) \rightarrow (19 \rightarrow)18 \rightarrow 1 \rightarrow C_6H_2 + H, \quad \Delta E = -92.1 \text{ kcal/mol},$$

$$CH(^2\Pi) + HCCCCCH(^3\Sigma_g^-) \rightarrow 6 \rightarrow C_6H_2 + H, \quad \Delta E = -100.8 \text{ kcal/mol},$$

$$CH_2(^3B_1) + 1 - C_5H(^2\Pi) \rightarrow 7 \rightarrow C_6H_2 + H, \quad \Delta E = -98.6 \text{ kcal/mol},$$

$$CH_3(^2A_2'') + C_5(^1\Sigma_g^+) \rightarrow 11 \rightarrow 10 \rightarrow 9 \rightarrow 8 \rightarrow 1 \rightarrow C_6H_2 + H, \quad \Delta E = -72.2 \text{ kcal/mol}.$$

Fine mechanistic details for these reactions await further investigation, which is beyond the scope of the present work. However, we can conclude here that, unless some of these reactions have an entrance barrier, all intermediates and TSs on the pathways to triacetylene+H lie significantly lower in energy than the initial reactants and thus C_6H_2+H can be easily formed.

Thermal rate constants of the $C_2H+C_4H_2$ reaction

Since the addition of ethynyl radical to C_4H_2 has no distinct barrier, thermal rate constants were computed using CVTST. We scanned the area of the C_6H_3 PES along the entrance channel of the $C_2H+C_4H_2$ reaction, i.e., in the region where C_2H approaches diacetylene and a new C—C bond is being formed. The calculations were carried out by changing the C—C distance (r_1 in Fig. 3) from 5.0 to 1.4 Å with the step size of 0.1 Å and the ∠CCC angle involving the attacking carbon atom of C_2H and two carbons of diacetylene from 180° with the step size of 1° to a value, at which the attacking C atom of C_2H becomes closer to the opposite end of the C_4H_2 molecule (where $r_2 < r_1$ in Fig. 3). Because of the symmetry of diacetylene, all possible approach trajectories of C_2H can be covered in such a way. All other geometric parameters in the C_6H_3 system were fully optimized. The calculations were performed at the B3LYP/6-311+G(*d*,*p*) level of theory. Next, for each par-

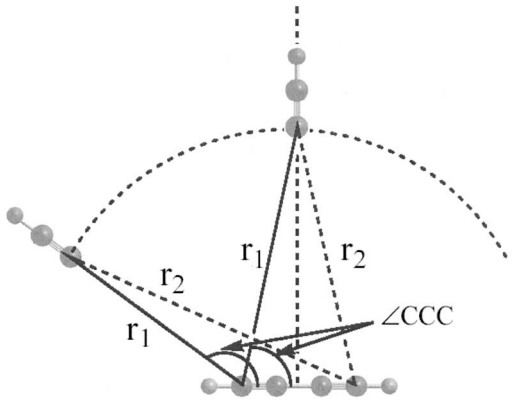

FIG. 3. Geometric scheme used for the scan of the C_6H_3 potential energy surface along the entrance channel of the $C_2H+C_4H_2$ reaction.

tially optimized structure on the grid (with fixed r_1 and the CCC angle), we computed $3N-7$ vibrational frequencies projecting the direction of the gradient out. The calculated molecular parameters of each structure, including frequencies and moments of inertia, and their relative energies with respect to the separated reactants were then used to compute relative Gibbs free energies ΔG with respect to separated $C_2H+C_4H_2$. To find the minimum Gibbs energy reaction pathway (MGEP) for each temperature, we looked for the structures with minimal ΔG value among those with the same r_1 but with different CCC angles,

$$\min_{CCC}[\Delta G(CCC)]|_{r_1,T}.$$

Then, we located variational TSs for different temperatures by searching for maximal values of

$$\min_{CCC}[\Delta G(CCC)]|_{r_1,T}$$

along MGEP, i.e., among different r_1 values,

$$\Delta G_{\text{max-min}}(T) = \max_{r_1}\{\min_{CCC}[\Delta G(CCC)]|_{r_1}\}|_T.$$

Finally, this max-min ΔG value was employed for the calculations of the following bimolecular thermal rate constants:

$$k = \left(\frac{RT}{P^{\varnothing}}\right)\frac{k_B T}{h} e^{-\Delta G_{\text{max-min}}(T)/RT},$$

where R is the Rydberg constant, k_B is the Boltzmann constant, h is the Planck constant, and $p^{\varnothing}$ is the standard pressure. It should be noted that the overall rate for the $C_2H+C_4H_2$ reaction can be represented to the first approximation by the rate of the initial association step. The H abstraction channel leading to $C_2H_2+C_4H$ is expected to be much slower because of the high barrier and the reverse reaction rate for highly exothermic barrierless addition reactions with at least one exothermic channel are normally negligible at low temperatures.[57,58]

The rate constants calculated in the temperature range of 63–298 K are shown in Fig. 4. They slightly decrease from 1.80×10^{-10} at the room temperature to 1.53×10^{-10} at 185 K and then rise to 6.85×10^{-10} at 63 K, with the sharpest increase found below 95 K (all rates are given in the units of cm^3 $molecule^{-1}$ s^{-1}). As no experimental rate constants so far are available for $C_2H+C_4H_2$, we carried out similar

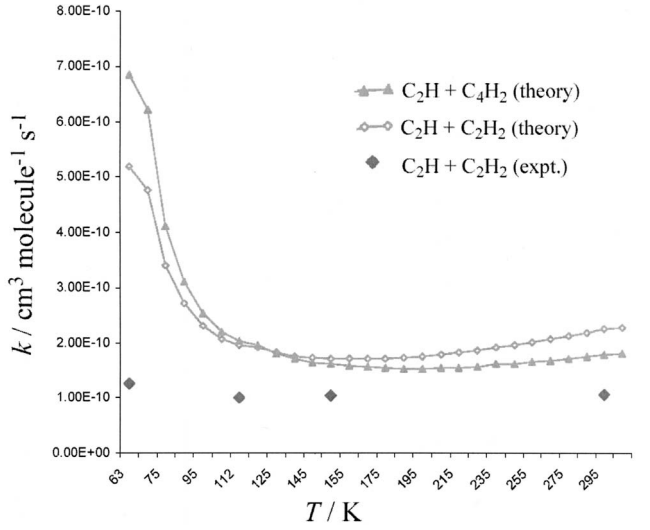

FIG. 4. Calculated thermal rate constants for the $C_2H+C_4H_2$ and $C_2H+C_2H_2$ reactions in comparison with experimental values for $C_2H+C_2H_2$ (from Ref. 34).

CVTST calculations for the $C_2H+C_2H_2$ reaction and compared the results to the experimental data by Chastaing *et al.*[34] (see Fig. 4). One can see that the agreement is within a factor of 2 for 112–298 K with the calculated values overestimating the experimental rate constants, but the deviation increases to a factor of 4 at 63 K. Apparently, the calculated rate constants for $C_2H+C_4H_2$ as well as for $C_2H+C_2H_2$ are less accurate at 63–95 K than at the higher temperatures. A probable reason for that is the fact that the computed rates at lower temperatures are much more sensitive with respect to small variations in molecular parameters and energetics. Theoretical rate constants for $C_2H+C_4H_2$ and their temperature dependence are found to be rather similar to those for $C_2H+C_2H_2$. The diacetylene reaction is calculated to be slightly slower than that of acetylene at 120–298 K but to become somewhat faster at the lower temperatures. Interestingly, for the related barrierless reaction of C_2H with benzene, Woon obtained rather similar rate constants of $(2.08–2.85)\times10^{-10}$ cm^3 $molecule^{-1}$ s^{-1} for the temperature range of 300–100 K using dynamical classical trajectory calculations,[58] whereas the experimental rates measured by Goulay and Leone were slightly higher, $(3.28–3.96)\times10^{-10}$ cm^3 $molecule^{-1}$ s^{-1}.[59]

We can also compare our CVTST $C_2H+C_2H_2$ and $C_2H+C_4H_2$ association rate constants to the values evaluated using long-range transition state theory developed by Georgievskii and Klippenstein.[60] In this approach, which should be most meaningful in the 10–100 K temperature range, one calculates dispersion, dipole-induced dipole, and dipole-quadrupole rata constants, and the largest of them provides a reasonable first approximation to the overall rate. The data needed for these calculations, the dipole moment of C_2H, quadruple moments of C_2H_2 and C_4H_2, and polarizabilities of C_2H, C_2H_2, and C_4H_2, were obtained at the B3LYP level with the augmented cc-pVTZ basis set, whereas ionization energies were taken from the NIST Chemistry Database.[61] The calculations show that for both systems the largest rate is due to dispersion. The evaluated dispersion rate constants

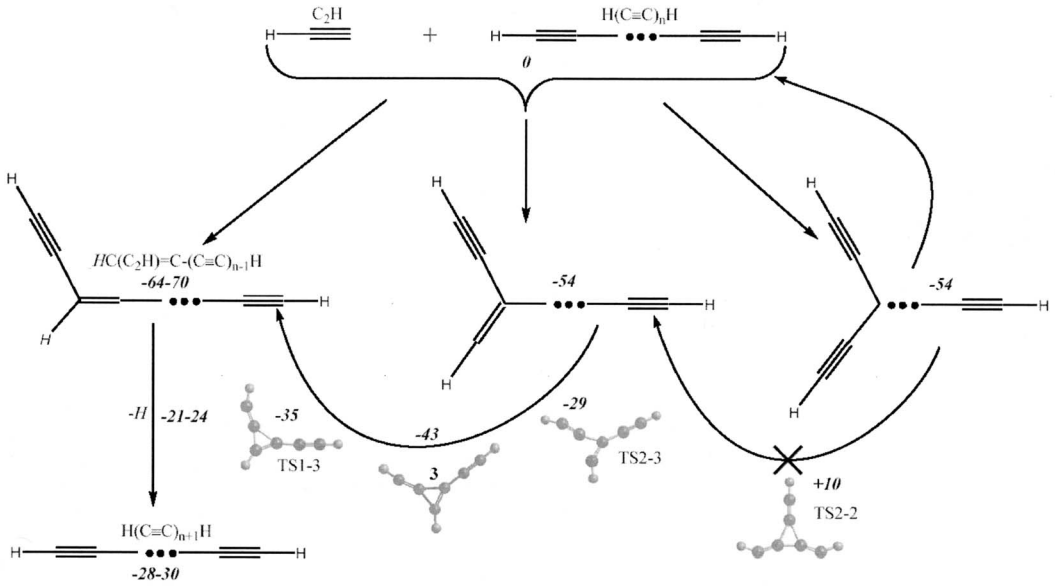

FIG. 5. Schematic presentation of possible mechanisms of the $C_2H+H(C{\equiv}C)_nH \rightarrow H(C{\equiv}C)_{n+1}H+H$ reactions. Bold italic numbers show relative energies (or estimated energy range) of various structures in kcal/mol.

increase in the 10–100 K temperature range from 3.52×10^{-10} to 5.16×10^{-10} cm^3 $molecule^{-1}$ s^{-1} for $C_2H+C_2H_2$ and from 3.88×10^{-10} to 5.69×10^{-10} cm^3 $molecule^{-1}$ s^{-1} for $C_2H+C_4H_2$; the higher rate estimates for diacetylene are caused by its higher polarizability, 50.01 $bohr^3$, as compared to 23.51 $bohr^3$ for acetylene. At 63 K, the CVTST and long-range TST values for $C_2H+C_2H_2$ closely agree, 5.19×10^{-10} versus 4.78×10^{-10} cm^3 $molecule^{-1}$ s^{-1}; the discrepancy is somewhat larger for $C_2H+C_4H_2$, 6.85×10^{-10} versus 5.27×10^{-10} cm^3 $molecule^{-1}$ s^{-1}, but the agreement is still reasonable.

Comparison of ethynyl reactions with acetylene and diacetylene and general mechanism for the growth of polyyne chains involving C_2H

We can now compare the mechanisms and rate constant for the first two reactions in series [Eq. (1)], $C_2H+C_2H_2 \rightarrow C_4H_2$ (diacetylene)+H and $C_2H+C_4H_2 \rightarrow C_6H_2$ (triacetylene)+H, and discuss most probable scenarios for the further growth of polyyne chains, $H(C{\equiv}C)_nH$. At the CCSD(T)/CBS level, both reactions are calculated to be similarly exothermic, by 28.3 and 29.7 kcal/mol, respectively. The initial step of C_2H addition to an acetylenic carbon occurs without an entrance barrier and is highly exothermic. In the reaction of ethynyl with acetylene, this step produces n-C_4H_3 with the energy gain of 59.7 kcal/mol, and in the case of diacetylene, the addition to a terminal C atom is preferable and leads to the formation of HCCCHCCCH with a higher exothermicity of 70.2 kcal/mol. Meanwhile, the C_2H addition to a middle carbon of diacetylene is less exothermic, by 53.9 kcal/mol, but also proceeds without a barrier. H elimination from n-C_4H_3 and HCCCHCCCH leads directly to the final products, di- or triacetylene, via the barriers of 38.3 and 45.8 kcal/mol (exit barriers of 9.0 and 5.3 kcal/mol), respectively. H migration barriers to eventually form the most stable C_4H_3 and C_6H_3 isomers H_2CCCCH (i-C_4H_3) and $H_2CCCCCCH$ 7 are calculated to be higher, 41.6 kcal/mol in the C_4H_3 system and 55.8 and 40.1 kcal/mol for the first and second H shift in C_6H_3. Thus, for both reactions, the simplest two-step C_2H-for-H exchange mechanisms, $C_2H+C_2H_2 \rightarrow n$-$C_4H_3 \rightarrow C_4H_2+H$ and $C_2H+C_4H_2 \rightarrow HCCCHCCCH \rightarrow C_6H_2+H$, are the most probable. This is supported by the results of RRKM calculations of branching ratios of different channels in the reactions. Summarizing, both C_2H reactions with acetylene and diacetylene are rather similar in terms of the mechanism, energetics, and rate constants, although the presence of two different types of C atoms in C_4H_2 adds some complexity.

Now, we can extrapolate the available information to reactions of ethynyl with longer polyyne chains $H(C{\equiv}C)_nH$. We can see that the initial C_2H addition is energetically preferable to the terminal carbon atoms of the chain to produce $HC(C_2H){=}C{-}(C{\equiv}C)_{n-1}H$ isomers of $C_{2n+2}H_3$ radicals (see Fig. 5). This step is expected to occur without a barrier and to be exothermic by about 70 kcal/mol. Next, elimination of hydrogen atom marked in italics in the $HC(C_2H)$ group should immediately give the final $H(C{\equiv}C)_{n+1}H$ product with an overall exothermicity of ~28–30 kcal/mol via an exit barrier of ~5 kcal/mol. H shifts in $HC(C_2H){=}C{-}(C{\equiv}C)_{n-1}H$, eventually leading to the more stable $H_2C_{2n+2}H$ intermediate, may compete with the H loss at each reaction step but are not expected to play a significant role.

Barrierless C_2H additions should also be possible to the other carbon atoms in the polyyne. In this case, exothermicity of the initial reaction step is anticipated to be somewhat lower, in the range of 50–60 kcal/mol. The carbon skeleton produced as a result of such additions will have a branched structure. Therefore, a direct H loss would lead to unfavorable branched $C_{2n+2}H_2$ isomers, and hence, is unlikely to be feasible. To produce the low energy polyyne $H(C{\equiv}C)_{n+1}H$ product, the branched $C_{2n+2}H_3$ intermediates will have to re-

arrange first to $HC(C_2H)=C-(C\equiv C)_{n-1}H$ or another chain isomer. Mechanistically, such a pathway has to involve C_2H migrations over C≡C and C—C bonds in the polyyne fragment. According to the results for the C_4H_3 and C_6H_3 systems, the migration over a C≡C bond takes place in two steps with cyclic structures such as HC-(c-C_3H_2) and 3, respectively, serving as intermediates. The barrier for C_2H migration over the C≡C bond is calculated to be 26.1 kcal/mol for C_4H_3 and 24.6 kcal/mol relative to the branched isomer 2 of C_6H_3. In both systems, the critical TSs reside about 30 kcal/mol below the initial reactants, rendering the C_2H shift facile. In larger systems, C_2H migration over a C—C bond will be additionally required to reach the $HC(C_2H)=C-(C\equiv C)_{n-1}H$ isomer. In C_6H_3, such migration corresponds to the degenerate $2\rightarrow 2$ rearrangement and occurs via the C_{2v}-symmetric TS illustrated in Fig. 5. However, the calculated barrier for this process is high, 64.1 kcal/mol, and the TS lies 10.2 kcal/mol above the $C_2H+C_4H_2$ reactants. This result indicates that the C_2H shift over a C—C bond is less favorable than elimination of the C_2H group leading back to the initial reactants. Thus, unless ethynyl adds to one of the two carbons in a terminal HC≡C unit, the reaction cannot lead to the enlarged polyyne $H(C\equiv C)_{n+1}H$ product, but rather returns to the $C_2H+H(C\equiv C)_nH$ reactants or dissociates to smaller fragments by cleaving a C—C single bond. This would probably result in a general decrease in the overall probability of the reactive $C_2H+H(C\equiv C)_nH\rightarrow H(C\equiv C)_{n+1}H+H$ collisions because only those C_2H attacks, which are directed toward the two terminal HC≡C groups, would lead to the products and the rest will recover the reactants.

CONCLUSIONS

Ab initio calculations of the C_6H_3 PES show that the reaction mechanism of ethynyl radical with diacetylene involves barrierless C_2H addition to an acetylenic C atom followed by H elimination. The initial step leads to the formation of either chain structure HCCCHCCCH 1, branched HCCC(CH)CCH 2, or three-member ring intermediate 3, which readily opens to produce the acyclic isomers. The most thermodynamically favorable entrance channel corresponds to the C_2H addition to a terminal carbon of C_4H_2 and produces HCCCHCCCH, residing 70.2 kcal/mol below the initial reactants. This adduct can lose a hydrogen atom from the nonterminal position to give the HCCCCCCH (triacetylene) product exothermic by 29.7 kcal/mol. The H elimination takes place with an exit barrier of 5.3 kcal/mol. The branched isomer 2 rearranges to 1 via 3 with highest in energy TS2-3 lying 29.3 kcal/mol below the reactants. The other reaction channels including direct H abstraction producing $C_2H_2+C_4H$, isomerization of 1 by hydrogen migrations or cyclization are not competitive. Triacetylene+H are concluded to be the exclusive reaction products (unless C_6H_3 intermediates are deactivated by collisions), and under single-collision conditions, more than 98% of these products are formed directly from 1. The $C_2H+C_4H_2$ reaction rate constants are calculated to be similar to those for $C_2H+C_2H_2$, in the order of magnitude of 10^{-10} cm^3 $molecule^{-1}$ s^{-1} for $T=298-63$ K, and to show negative temperature dependence at low T.

Other regions of the C_6H_3 PES can be accessed by different bimolecular reactions but all of them are predicted to produce HCCCCCCH+H barring collisional stabilization. For instance, $C_4H+C_2H_2$ first yields the HCCHCCCCH intermediate 6 without a barrier, which either loses H from the nonterminal C atom directly or rearranges to the most stable chain C_6H_3 isomer $H_2CCCCCCH$ 7. About two thirds of the triacetylene products in the C_4H+C_2H reaction are expected to be formed from 6, with the rest mostly coming from 7. The 1,2,3- and 1,2,4-tridehydrobenzene C_6H_3 isomers 12 and 13 are nearly isoergic with $H_2CCCCCCH$, with 12 calculated to be 1.5 kcal/mol lower and 13 calculated to be −0.6 kcal/mol higher in energy than 7 at the CCSD(T)/CBS level. The six-member ring isomers can be accessed by H loss from benzyne C_6H_4 and are predicted to undergo unimolecular decomposition to triacetylene+H under thermal conditions with the highest barriers on the reaction pathways being ~66 and ~51 kcal/mol for 12 and 13, respectively.

ASTROPHYSICAL IMPLICATIONS

The results of the theoretical investigations have important implications to the chemical evolution of hydrocarbon-rich atmospheres of planets and their moons as well as of the chemical processing of the interstellar medium (ISM). Our computations, which still have to be verified by crossed molecular beams experiments, suggest that in the atmosphere of Saturn's moon Titan, the triacetylene molecule (HCCCCCCH) can be formed by exoergic and barrierless reactions of butadiynyl radicals (CCCCH) with acetylene (HCCH) and/or of ethynyl radicals (HCC) with diacetylene (HCCCCH) under single-collision conditions. It should be stressed that these bimolecular reactions are also of relevance to the ongoing chemistry in the ISM. Here, utilizing the Infrared Space Observatory (ISO), Cernicharo *et al.* discovered the polyacetylenic chains diacetylene and triacetylene toward the protoplanetary nebulas CRL 618 and CRL 2688.[62] Surprisingly, the abundances of di- and triacetylene are only a factor of 2–4 lower than that of acetylene. The authors suggested that ultraviolet photons could photodissociate acetylene into ethynyl radicals plus atomic hydrogen. In successive reactions, ethynyl radicals could buildup diacetylene and triacetylene. Our computations studies fully verify this hypothesis. Therefore, it is highly likely that diacetylene and triacetylene are formed by bimolecular neutral-neutral reactions involving at least ethynyl radicals in the protoplanetary nebulas CRL 618 and CRL 2688.

ACKNOWLEDGMENTS

This work was funded by the Collaborative Research in Chemistry (CRC) Program of the National Science Foundation (Award No. CHE-0627854).

[1] N. Sarker, A. Somogyi, J. I. Lunine, and M. A. Smith, Astrobiology **3**, 719 (2003).
[2] R. A. Kerr, Science **307**, 330 (2005); E. Wilson, Chem. Eng. News **83**, 6 (2005).
[3] Y. L. Yung, M. Allen, and J. P. Pinto, Astrophys. J., Suppl. Ser. **55**, 465 (1984).
[4] B. Letourneur and A. Coustenis, Planet. Space Sci. **41**, 593 (1993); T. Hidayat, A. Marten, B. Bezard, D. Gautier, T. Owen, H. E. Matthews, and G. Paubert, Icarus **133**, 109 (1998).
[5] R. A. Marcus, J. Chem. Phys. **121**, 8201 (2004).
[6] D. W. Clarke and J. P. Ferris, Icarus **127**, 158 (1997); T. Hidayat, A. Marten, B. Bezard, T. Owen, H. E. Matthews, and G. Paubert, *ibid.* **126**, 170 (1997).
[7] J. I. Lunine, Y. L. Yung, and R. D. Lorenz, Planet. Space Sci. **47**, 1291 (1999).
[8] M. A. Gurwell, Astrophys. J. Lett. **616**, L7 (2004).
[9] A. S. Wong, C. G. Morgan, Y. L. Yung, and T. Owen, Icarus **155**, 382 (2002).
[10] J. H. Waite, Jr., H. Niemann, R. V. Yelle, W. T. Kasprzak, T. E. Cravens, J. G. Luhmann, R. L. McNutt, W.-H. Ip, D. Gell, V. De La Haye, I. Mueller-Wordag, B. Magee, N. Borggren, S. Ledvina, G. Fletcher, E. Walter, R. Miller, S. Scherer, R. Thorpe, J. Xu, B. Block, and K. Arnett, Science **308**, 982 (2005).
[11] Y. L. Yung and W. D. De More, *Photochemistry of Planetary Atmospheres* (Oxford University Press, Oxford, 1999).
[12] A.-S. Wong, Y. L. Yung, and A. J. Friedson, Geophys. Res. Lett. **30**, 1447, DOI:10.1029/2002GL016661 (2003).
[13] E. H. Wilson and S. K. Atreya, Planet. Space Sci. **51**, 1017 (2003).
[14] W. M. Jackson and A. Scodinu, Astrophys. Space Sci. Lib. **311**, 85 (2004); G. Apaydin, W. H. Fink, and W. M. Jackson, J. Chem. Phys. **121**, 9368 (2004); N. S. Smith and F. Raulin, J. Geophys. Res. **104**, 1873, DOI:10.1029/1998JE900027 (1999).
[15] N. S. Smith, Y. Benilan, and P. Bruston, Planet. Space Sci. **46**, 1215 (1998).
[16] J. H. Wang, K. Liu, Z. Min, H. Su, R. Bersohn, J. Preses, and J. Z. Larese, J. Chem. Phys. **113**, 4146 (2000).
[17] R. J. Cody, P. N. Romani, F. L. Nesbitt, M. A. Iannone, D. C. Tardy, and L. J. Stief, J. Geophys. Res. **108**, 5119, DOI:10.1029/2002JE002037 (2003); R. J. Cody, W. A. Payne, Jr., R. P. Thorn, Jr., F. L. Nesbitt, M. A. Iannone, D. C. Tardy, and L. J. Stief, J. Phys. Chem. A **106**, 606 (2002); G. P. Smith, Chem. Phys. Lett. **376**, 381 (2003); M. J. Davis and S. J. Klippenstein, J. Phys. Chem. A **106**, 5860 (2002).
[18] K. Seki and H. Okabe, J. Phys. Chem. **97**, 5284 (1993); B. A. Balko, J. Zhang, and Y. T. Lee, J. Chem. Phys. **94**, 7958 (1991); A. Läuter, K. S. Lee, K. H. Jung, R. K. Vatsa, J. P. Mittal, and H.-R. Volpp, Chem. Phys. Lett. **358**, 314 (2002); A. M. Wodtke and Y. T. Lee, J. Phys. Chem. **89**, 4744 (1985); J. Segall, Y. Wen, R. Lavi, R. Singer, and C. Wittig, *ibid.* **95**, 8078 (1991); H. Okabe, J. Chem. Phys. **78**, 1312 (1983).
[19] S.-H. Lee, Y. T. Lee, and X. Yang, J. Chem. Phys. **120**, 10983 (2004); E. F. Cromwell, A. Stolow, M. J. J. Vrakking, and Y. T. Lee, *ibid.* **97**, 4029 (1992); B. A. Balko, J. Zhang, and Y. T. Lee, *ibid.* **97**, 935 (1992); A. H. H. Chang, A. M. Mebel, X.-M. Yang, S. H. Lin, and Y. T. Lee, Chem. Phys. Lett. **287**, 301 (1998); J. J. Lin, D. W. Hwang, Y. T. Lee, and X. Yang, J. Chem. Phys. **109**, 2979 (1998); A. Peña-Gallergo, E. Martínez-Núñez, and S. A. Vázquez, Chem. Phys. Lett. **353**, 418 (2002).
[20] M. Allen, J. P. Pinto, and Y. L. Yung, Astrophys. J. **242**, L125 (1980).
[21] L. M. Lara, E. Lellouch, J. J. Lopez-Moreno, and R. Rodrigo, J. Geophys. Res. **101**, 23261, DOI:10.1029/96JE02036 (1996).
[22] M. C. Gazeau, H. Cottin, V. Vuitton, N. Smith, and F. Raulin, Planet. Space Sci. **48**, 437 (2000).
[23] C. N. Keller, V. G. Anicich, and T. E. Cravens, Planet. Space Sci. **46**, 1157 (1998).
[24] M. Banaszkiewicz, L. M. Lara, R. Rodrigo, J. J. Lopez-Moreno, and G. J. Molina-Cuberos, Icarus **147**, 386 (2000); P. Rannou, F. Hourdin, C. P. McKay, and D. Luz, *ibid.* **170**, 443 (2004).
[25] D. Toublanc, J. P. Parisot, J. Brillet, D. Gautier, F. Raulin, and C. P. McKay, Icarus **113**, 2 (1995); L. M. Lara, E. Lellouch, and V. Shematovich, Astron. Astrophys. **341**, 312 (1999).
[26] E. H. Wilson and S. K. Atreya, J. Geophys. Res. **109**, E06002, DOI:10.1029/2003JE002181 (2004).
[27] R. D. Lorenz, C. P. McKay, and J. I. Lunine, Science **275**, 642 (1997).
[28] E. H. Wilson, S. K. Atreya, and A. Coustenis, J. Geophys. Res. **108**, 5014, DOI:10.1029/2002JE001896 (2003).
[29] T. L. Roush and J. B. Dalton, Icarus **168**, 158 (2004).
[30] R. Lorenz and J. Mitton, *Lifting Titan's Veil* (Cambridge University Press, Cambridge, 2002).
[31] J. O. P. Pedersen, B. J. Opansky, and S. R. Leone, J. Phys. Chem. **97**, 6822 (1993).
[32] H. Van Look and J. Peeters, J. Phys. Chem. **99**, 16284 (1995).
[33] B. Ceursters, H. M. T. Nguyen, J. Peeters, and M. T. Nguyen, Chem. Phys. **262**, 243 (2000).
[34] D. Chastaing, P. L. James, I. R. Sims, and I. W. M. Smith, Faraday Discuss. **109**, 165 (1998).
[35] R. I. Kaiser, F. Stahl, P. v. R. Schleyer, and H. F. Schaefer III, Phys. Chem. Chem. Phys. **4**, 2950 (2002).
[36] T. N. Le, A. M. Mebel, and R. I. Kaiser, J. Comput. Chem. **22**, 1522 (2001).
[37] R. K. Frost, G. S. Zavarin, and T. S. Zwier, J. Phys. Chem. **99**, 9408 (1995).
[38] C. Xu, M. Braun-Unkhoff, C. Naumann, and P. Frank, Proc. Combust. Inst. **31**, 231 (2007).
[39] Y. Guo, X. Gu, F. Zhang, A. M. Mebel, and R. I. Kaiser, Phys. Chem. Chem. Phys. **9**, 1972 (2007).
[40] H. F. Bettinger, P. v. R. Schleyer, and H. F. Schaefer III, J. Am. Chem. Soc. **121**, 2829 (1999).
[41] H. M. T. Nguyen, T. Holtzl, G. Gopakumar, T. Veszpremi, J. Peeters, and M. T. Nguyen, Chem. Phys. **316**, 125 (2005).
[42] A. D. Becke, J. Chem. Phys. **98**, 5648 (1993).
[43] C. Lee, W. Yang, and R. G. Parr, Phys. Rev. B **37**, 785 (1988).
[44] See EPAPS Document No. E-JCPSA6-128-001822 for optimized geometries, rotational constants, vibrational frequencies, and total B3LYP/6-311G** energies and ZPE of all species on the C_6H_3 PES. For more information on EPAPS, see http://www.aip.org/pubservs/epaps.html.
[45] G. D. Purvis and R. J. Bartlett, J. Chem. Phys. **76**, 1910 (1982); G. E. Scuseria, C. L. Janssen, and H. F. Schaefer III, *ibid.* **89**, 7382 (1988); G. E. Scuseria and H. F. Schaefer III, *ibid.* **90**, 3700 (1989); J. A. Pople, M. Head-Gordon, and K. Raghavachari, *ibid.* **87**, 5968 (1987).
[46] T. H. Dunning, Jr., J. Chem. Phys. **90**, 1007 (1989).
[47] K. A. Peterson and T. H. Dunning, Jr., J. Chem. Phys. **99**, 3898 (1995).
[48] K. M. Ervin, S. Gronert, S. E. Barlow, M. K. Gilles, A. G. Harrison, V. M. Beirbaum, C. H. DePuy, W. C. Lineberger, and G. B. Ellison, J. Am. Chem. Soc. **112**, 5750 (1990).
[49] M. J. Frisch, G. W. Trucks, H. B. Schlegel *et al.*, GAUSSIAN 98, Revision A.9, Gaussian, Inc., Pittsburgh, PA, 1998.
[50] MOLPRO, a package of *ab initio* programs written by H.-J. Werner and P. J. Knowles, Version 2002.6, R. D. Amos et al., University of Birmingham: Birmingham, UK, 2003.
[51] M. Sayes, M.-F. Reyniers, G. B. Marin, V. Van Speybroeck, and M. Waroquier, J. Phys. Chem. A **107**, 9147 (2003).
[52] D. K. Malick, G. A. Petersson, and J. A. Montgomery, J. Chem. Phys. **108**, 5704 (1998).
[53] V. V. Kislov, T. L. Nguyen, A. M. Mebel, S. H. Lin, and S. C. Smith, J. Chem. Phys. **120**, 7008 (2004).
[54] A. M. Mebel, M. C. Lin, D. Chakraborty, J. Park, S. H. Lin, and Y. T. Lee, J. Chem. Phys. **114**, 8421 (2001).
[55] L. K. Madden, L. V. Moskaleva, S. Kristyan, and M. C. Lin, J. Phys. Chem. A **101**, 6790 (1997).
[56] L. V. Moskaleva, L. K. Madden, and M. C. Lin, Phys. Chem. Chem. Phys. **1**, 3967 (1999).
[57] J. Troe and V. G. Ushakov, J. Chem. Phys. **115**, 3621 (2001).
[58] D. E. Woon, Chem. Phys. **331**, 67 (2006).
[59] F. Goulay and S. R. Leone, J. Phys. Chem. A **110**, 1875 (2006).
[60] Y. Georgievskii and S. J. Klippenstein, J. Chem. Phys. **122**, 194103 (2005).
[61] P. J. Linstrom, in *NIST Chemistry WebBook*, NIST Standard Reference Database Number 69, edited by W. G. Mallard (National Institute of Standards and Technology, Gaithersburg, 2003), http://webbook.nist.gov/chemistry/.
[62] J. Cernicharo, A. M. Heras, A. G. G. M. Tielens, J. R. Pardo, F. Herpin, M. Guélin, and L. B. F. M. Waters, Astrophys. J. **546**, L123 (2001).